Cytotoxic and Optically Active Pyrisulfoxins From the Endophytic *Streptomyces albolongus* EA12432

Yuqi Du[1†], Chen Wang[1†], Guodong Cui[1†], Yiwen Chu[2], Qian Jia[1], Yi Wang[1*] and Weiming Zhu[1,3*]

[1] Key Laboratory of Marine Drugs, Ministry of Education of China, School of Medicine and Pharmacy, Ocean University of China, Qingdao, China, [2] Sichuan Industrial Institute of Antibiotics, Sichuan Industrial Institute of Antibiotics, Chengdu University, Chengdu, China, [3] Laboratory for Marine Drugs and Bioproducts of Pilot National Laboratory for Marine Science and Technology, Qingdao, China

R-Pyrisulfoxin C (**1**), *S*-pyrisulfoxin D [(+)-**2**], *R*-pyrisulfoxin D [(–)-**2**], pyrisulfoxin E (**13**), *S*-pyrisulfoxin F [(+)-**14**], and *R*-pyrisulfoxin F [(–)-**14**], six new caerulomycin derivatives with a 2,2′-bipyridine skeleton, were obtained from the cultures of the endophytic *Streptomyces albolongus* EA12432 with *Aconitum carmichaeli* (Ranunculaceae). Additionally, the racemic pyrisulfoxins A [(±)-**3**] and B [(±)-**4**] were further purified as optically pure compounds and identified the configurations for the first time. The racemic pyrisulfoxin D [(±)-**2**] displayed significant cytotoxicity against a series of cancer cell lines with IC_{50} values ranging from 0.92 to 9.71 μM. Compounds **7**, **8**, and (±)-**3** showed cytotoxicity against the HCT-116, HT-29, BXPC-3, P6C, and MCF-7 cell lines. Notably, compounds **7** and **8** have a strong inhibition both on the proliferation of human colon cancer cells HCT-116 and HT-29 with IC_{50} values ranging from 0.048 to 0.2 μM (doxorubicin, 0.21 and 0.16 μM), and compound **1** showed a selective inhibition on the proliferation of the gastric carcinoma cell lines, N87, with an IC_{50} value of 8.09 μM. Optically pure compounds *R*(–)-**14** and *S*(+)-**14** showed weak cytotoxicity against HCT-116 and MCF-7 cell lines with the IC_{50} values of 14.7 μM and 10.4 μM, respectively. Interestingly, compounds **1** and (±)-**2** didn't show cytotoxic activity against two human normal cell lines, HEK-293F and L02, with IC_{50} values >100 μM.

Keywords: 2,2′-bipyridine, cytotoxicity, endophyte, *Streptomyces albolongus*, *Aconitum carmichaeli*

INTRODUCTION

Caerulomycin A is an alkaloid with a 2,2′-bypyridine core, firstly discovered from the cultures of strain *Streptomyces caeruleus* in 1959 (Funk and Divekar, 1959). Since then, large amounts of its analogs or derivatives have been isolated from both wild and mutant actinomycetes, such as caerulomycins (CAEs) (Gomi et al., 1994), collimycins (COLs) (Shindo et al., 1994), and pyrisulfoxins (PYRs) (Tsuge et al., 1999). All of these compounds consist of a 2-substituted pyridine and a tri- or tetra-substituted pyridine ring system, which were also called 2,2′-bipyridine derivatives. 2,2′-Bipyridine derivatives are well-known for their antibacterial (Ambavane et al., 2014; Bu et al., 2014), immunosuppressant (Gurram et al., 2014; Kujur et al., 2015, 2017), and cytotoxic activities (Fu et al., 2011a, 2014; Mei et al., 2019). Our group has reported cytotoxic CAE compounds, cyanogrisides A–N (Fu et al., 2011a, 2014; Mei et al., 2019), CAEs F–K (Fu et al., 2011b), and CAEs T–W (Mei et al., 2019) against several tumor cells, from *Actinoalloteichus*

GRAPHICAL ABSTRACT | Six new caerulomycin derivatives were obtained from the endophytic Streptomyces albolongus EA12432 by solid culture.
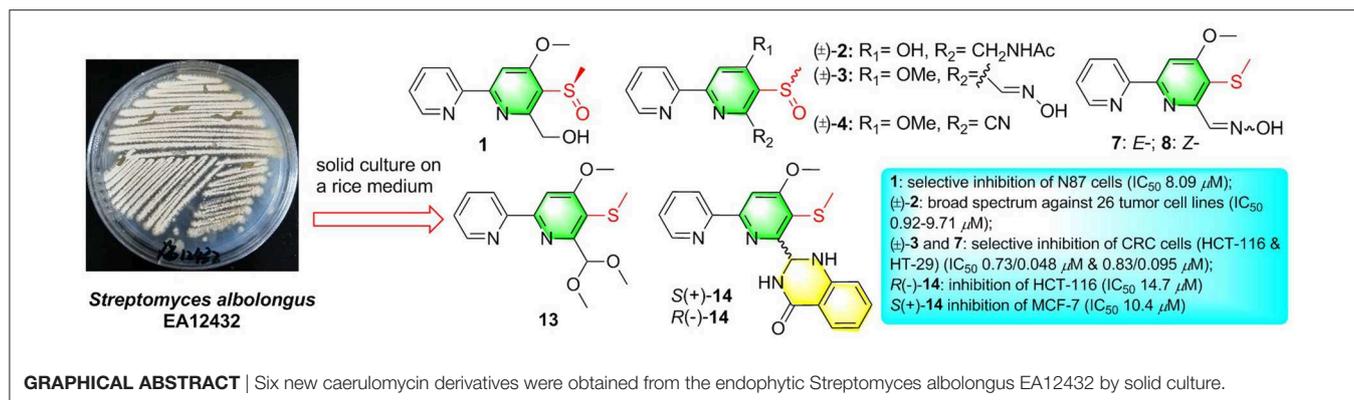
cyanogriseus WH1-2216-6. In our ongoing research, we identified three new PYRs containing a methyl sulfoxide group, pyrisulfoxin C (**1**), (+)-pyrisulfoxin D [(+)-**2**], and (−)-pyrisulfoxin D [(−)-**2**], along with the known analogs **3**–**11** and their biosynthetic precursor, picolinic acid (**12**) (**Tables S1, S2**) (Mehler, 1956), from a rice culture of the endophytic *Streptomyces albolongus* EA12432 isolated from *Aconitum carmichaeli* (Ranunculaceae), a famous Chinese medicinal plant (Yin et al., 2016). When the culture time was extended to 90 d, apart from the isolated compounds **1** and **3**–**11** from 30 d cultures, three new different PYRs, pyrisulfoxin E (**13**), (+)-pyrisulfoxin F [(+)-**14**], and (−)-pyrisulfoxin F [(−)-**14**], were identified (**Figure S53**). The known analogs included (±)-pyrisulfoxins A [(±)-**3**] and B [(±)-**4**] (Tsuge et al., 1999; Lee et al., 2017), which were further chirally resolved as their optically pure isomers for the first time, *N*-[(4-hydroxy-5-methylthio-2,2′-bipyridin-6-yl)methyl] acetamide (**5**) (**Tables S1, S2**) (Ignacio et al., 2012) and SF2738 A–F (**6**–**11**) (**Tables S1–S3**) (Gomi et al., 1994; Yin et al., 2016). The absolute configurations of pyrisulfoxin C (**1**), *S*(+)-**2**, *S*(+)-**3**, *S*(+)-**4**, *R*(−)-**2**, *R*(−)-**3**, and *R*(−)-**4** were determined by experimental and calculated electronic circular dichroism (ECD) spectra. Compounds **1**, (±)-**2**, (±)-**3**, **7**, and **8** displayed significant cytotoxicity against cancer cells with the IC$_{50}$ values ranging from 0.048 to 9.71 μM. Compounds *R*(−)-**14** and *S*(+)-**14** showed inhibitory activity against HCT-116 and MCF-7 cancer cell lines with the IC$_{50}$ values of 14.7 and 10.4 μM, respectively.

Notably, compounds **1**–**4** all bare a methyl sulfoxide group in the 2,2′-bypyridine nuclei. By searching the key words of "natural products (NPs) with sulfoxide" in SciFinder database, about 136 NPs baring sulfoxide group were reported. Apart from numerous sulfoxide-containing NPs from allium plants (Nohara et al., 2012, 2013; Edmands et al., 2013; Radulović et al., 2015; Fukaya et al., 2017), some sulfoxide-containing peptides and β-carboline derivatives, were isolated from marine sponge and ascidian, respectively. The methyl sulfoxide-containing peptides include cytotoxic haligramides A and B (Rashid et al., 2000), hymenamide F (Kobayashi et al., 1996), ciliatamide D (Imae et al., 2013; Takada et al., 2017), waiakeamide (Mau et al., 1996) and its sulfone derivative (Sera et al., 2003), as well as polytheonamides A and B (Hamada et al., 2005). The methyl sulfoxide-containing β-carboline derivatives include eudistomin E (Murata et al., 1991),

didemnolines C and D (Schumacher and Davidson, 1995), and eudistomin K sulfoxide with antiviral activity (Lake et al., 1988). Also, a series of sulfoxides with potent cytotoxicity were isolated from microorganisms, including leinamycin (Kara et al., 1989), apratoxin A sulfoxide (Thornburg et al., 2013), and quinomycin derivatives RK-1355 A and B (Lim et al., 2014).

MATERIALS AND METHODS

General Experimental Procedures

Melting points were obtained on X-4 digital display micro-melting point measuring instrument. Optical rotations were measured with POLAX-L polarimeter. Ultraviolet (UV) spectra were recorded on a Thermo Fisher Scientific NanoDrop One micro-spectrophotometer. IR spectra were taken on a Nicolet Nexus 470 spectrophotometer using KBr pellets. ECD spectra were measured on a JASCO-815 spectrometer (JASCO, Tokyo, Japan). Nuclear magnetic resonance (NMR) spectra of compounds **1**, **2**, and **4**–**13** were recorded on a Bruker Avance 500 MHz spectrometer while **2a**, **3**, and **14**, were measured on a JEOL JNM-ECP 600 spectrometer with TMS as an internal standard. Chemical shift (δ) was expressed in ppm with reference to the solvent signals. Mass spectra were recorded on an Agilent 6200 Q-TOF MS system. Thin layer chromatography (TLC) was performed on plates precoated with silica gel GF$_{254}$ (10–40 μm). Column chromatography (CC) was performed on silica gel (100–200 mesh, 200–300 mesh, 300–400 mesh, Qingdao Marine Chemical Ltd., Qingdao, People's Republic of China), RP-18 gel (20–45 μm), and Sephadex LH-20 (Amersham Biosciences). Medium-pressure liquid chromatography (MPLC) was performed on a LC3000 equipped with a P3000A pump modules, and columns packed with RP-18 gel. Semi-preparative high-performance liquid chromatography (HPLC) was performed using an octadecyl silica (ODS) column [YMC-pack ODS-A, 10 × 250 mm, 5 μm, 4 ml/min].

Actinobacterial Material

The endophytic actinobacterium strain EA12432 was isolated from *Aconitum carmichaeli* (Ranunculaceae) and identified as *Streptomyces albolongus* by 16S rRNA gene sequence and morphological characteristics (Yin et al., 2016).

Fermentation and Extraction

Spores were inoculated into 500 ml Erlenmeyer flasks containing 150 ml liquid medium that was prepared by dissolving soluble starch (20 g), KNO_3 (1 g), $K_2HPO_4 \cdot 3H_2O$ (0.5 g), $MgSO_4 \cdot 7H_2O$ (0.5 g), $FeSO_4$ (0.01 g), and NaCl (0.5 g) in sea water (1L). The flasks were incubated at 180 rpm and 28°C for 5 days as seed culture (OD_{600} 1.375), which was then inoculated into 200 × 1,000 ml Erlenmeyer flasks, each containing 80 g rice and 40 ml sea water. All the media were statically cultured at 28°C for 30 d. The culture broth was extracted with ethyl acetate (EtOAc) four times (30 L each). The EtOAc extracts were concentrated under reduced pressure to yield a dark brown gum 30 (40.2 g).

Spores were inoculated into 500 ml Erlenmeyer flasks containing 150 ml liquid medium that was prepared by dissolving soluble starch (20 g), KNO_3 (1 g), $K_2HPO_4 \cdot 3H_2O$ (0.5 g), $MgSO_4 \cdot 7H_2O$ (0.5 g), $FeSO_4$ (0.01 g), and NaCl (0.5 g) in sea water (1L). The flasks were incubated at 180 rpm and 28°C for 5 days as seed culture (OD_{600} 1.504), which was then inoculated into 1,000 ml Erlenmeyer flasks containing 80 g rice and 40 ml sea water. The flasks were incubated at room temperature for 90 d. The culture broth was soaked and extracted with ethyl acetate (EtOAc) four times (30 L each). The EtOAc extracts were concentrated under reduced pressure to yield a dark brown gum 90 (10 g).

Isolation

The gum 30 (40.2 g) was separated on silica gel using stepwise gradient elution with ethyl acetate/petroleum ether (0–100%) followed by $MeOH/CH_2Cl_2$ (0–10%) to yield 12 fractions (30 Fr.1–30 Fr.12). 30 Fr.8 (4.46 g) was separated by column chromatography on silica gel using stepwise gradient elution with $CH_2Cl_2/MeOH$ (300:1–1:1) to yield eight fractions (30 Fr.8-1–30 Fr.8-8) and 7 (97 mg). 30 Fr.8-1 (818.8 mg) was further separated into three subfractions on Sephadex LH-20, eluting with $CH_2Cl_2/MeOH$ (1:1). 30 Fr.8-1-2 (539 mg) was separated on an ODS column eluting with $MeOH/H_2O$ (10–100%) to give 8 (17.4 mg) and 9 (90.6 mg). 30 Fr.8-1-3 (86.8 mg) was subjected to an ODS column eluting with $MeOH/H_2O$ (10–100%) to give compound 12 (57.1 mg). 30 Fr.8-8 (60.7 mg) was purified by semi-preparative HPLC on an ODS column (65% $MeOH/H_2O$) to yield 10 (32.6 mg, t_R 11.5 min) and 11 (14.2 mg, t_R 16.5 min). Fr.10 (2.54 g) was subjected to Sephadex LH-20 using MeOH to afford six subfractions (30 Fr.10-1–30 Fr.10-6). 30 Fr.10-5 (958.9 mg) was further separated by VLC on silica gel eluting with petroleum ether/ethyl acetate (10:1–1:1). 30 Fr.10-5-7 (266.2 mg) was further separated into six subfractions (30 Fr.10-5-7-1–30 Fr.10-5-7-6) on silica gel using stepwise gradient elution with petroleum ether/EtOAc (3:1–1:1). 30 Fr.10-5-7-2 (182 mg) was separated on Sephadex LH-20, eluting with $CH_2Cl_2/MeOH$ (1:1), among which the second subfraction, 30 Fr.10-5-7-2-2 (70.3 mg) was purified by a preparative MPLC over an ODS column (25% $MeCN/H_2O$) to yield 1 (48.3 mg, t_R 4.0 min), (±)-4 (2.1 mg, t_R 8.5 min), and 6 (7.2 mg, t_R 12.5 min). (±)-4 was further separated into (+)-4 (0.9 mg, t_R 10.8 min) and (−)-4 (1.7 mg, t_R 12.0 min) on a ChiralPak IA analytical column (40% EtOH/*n*-hexane). 30 Fr.10-5-8 (700 mg) were separated on Sephadex LH-20, eluting with $CH_2Cl_2/MeOH$ (1:1). Fr.10-5-8-2

(450 mg) was separated into 10 subfractions (30 Fr.10-5-8-2-1– 30 Fr.10-5-8-2-10) on silica gel using stepwise gradient elution with $CH_2Cl_2/MeOH$ (40:1–1:1). 30 Fr.10-5-8-2-4 (151.7 mg) was then purified by semi-preparative HPLC (20% $MeCN/H_2O$) to yield (±)-3 (6.5 mg, t_R 23.0 min), which was further separated into (+)-3 (2.1 mg, t_R 8.0 min) and (−)-3 (1.6 mg, t_R 9.5 min) on a ChiralPak IA analytical column (35% EtOH/*n*-hexane). 30 Fr.10-5-8-2-5 (85.1 mg) was purified by MPLC (20% $MeCN/H_2O$, ODS-A C18 column) to yield (±)-2 (10 mg, t_R 4.5 min), along with 5 (25.1 mg, t_R 7.8 min). (±)-2 was further separated into (+)-2 (1.3 mg, t_R 21.0 min) and (−)-2 (1.7 mg, t_R 24.0 min) on a Chiral tris(3,5-dimethylphenylcarbamate) immobilized cellulose (INB) analytical column (20% EtOH/*n*-hexane/Et_2NH).

The gum 90 (10 g) was subjected to a silica gel column, eluted by stepwise gradient of ethyl acetate/petroleum ether (0–100%) followed by $MeOH/CH_2Cl_2$ (0–10%) to yield 13 fractions (90 Fr.1–90 Fr.13). 90 Fr.11 (300 mg) was separated on a Sephadex LH-20 column eluted by MeOH to give five subfractions, 90 Fr.11-1–90 Fr.11-5. 90 Fr.11-2 (40 mg) was further separated by semi-preparative HPLC (65% $MeOH/H_2O$, YMC-ODS column) to yield compound 13 (2.5 mg, t_R 9.0 min). 90 Fr.12 (400 mg) was separated on a Sephadex LH-20 column eluted by MeOH to provide three subfractions, 90 Fr.12-1–90 Fr.12-3. 90 Fr.12-2 (100 mg) was further separated by semi-preparative HPLC (60% $MeOH/H_2O$, YMC-ODS column) to yield (±)-14 (3.0 mg, t_R 8.0 min), which was resolved into (+)-14 (1.2 mg, t_R 22.0 min) and (−)-14 (1.1 mg, t_R 16.0 min) on a ChiralPak IA analytical column (30% *i*-PrOH/*n*-hexane).

R-Pyrisulfoxin C (1): white amorphous powder; $[\alpha]_D^{13}$ −33.4 (*c* 0.5, MeOH); UV(MeOH) λ_{max} (log ε) 249 (3.57), 289 (3.81) nm; IR (KBr) ν_{max} 3,346, 2,922, 1,569, 1,464, 1,422, 1,374, 1,039, 957, 798 cm^{-1}; ECD (0.90 mM, MeOH) λ_{max} ($\Delta\varepsilon$) 216 (+5.5), 243 (+2.9), and 291 (−3.9) nm; ^{1}H NMR and ^{13}C NMR, see **Tables 1**, **3**. High Resolution Electrospray Ionization Mass Spectroscopy (HRESIMS) *m/z* 279.0795 [M + H]$^+$ (calcd for $C_{13}H_{15}N_2O_3S$, 279.0798).

S-Pyrisulfoxin D [(+)-2]: white amorphous powder; $[\alpha]_D^{13}$ +14.2 (*c* 0.5, MeOH); UV(MeOH) λ_{max} (log ε) 242 (4.49), 282 (4.28) nm; IR (KBr) ν_{max} 3,260, 3,053, 2,922, 1,631, 1,572, 1,493, 1,383, 1,290, 1,029, 794 cm^{-1}; ECD (0.82 mM, MeOH) λ_{max} ($\Delta\varepsilon$) 221 (−12.8), 250 (+9.4), and 300 (+5.3) nm; ^{1}H NMR and ^{13}C NMR, see **Tables 1**, **3**. HRESIMS *m/z* 306.0916 [M + H]$^+$ (calcd for $C_{14}H_{16}N_3O_3S$, 306.0907).

R-Pyrisulfoxin D [(−)-2]: white amorphous powder; $[\alpha]_D^{13}$ −16.6 (*c* 0.5, MeOH); UV(MeOH) λ_{max} (log ε) 242 (4.49), 282 (4.28) nm; IR (KBr) ν_{max} 3,260, 3,053, 2,922, 1,631, 1,572, 1,493, 1,383, 1,290, 1,029, 794 cm^{-1}; ECD (0.82 mM, MeOH) λ_{max} ($\Delta\varepsilon$) 220 (+9.7), 250 (−7.7), and 300 (−3.4) nm; ^{1}H NMR and ^{13}C NMR, see **Tables 1**, **3**. HRESIMS *m/z* 306.0916 [M + H]$^+$ (calcd for $C_{14}H_{16}N_3O_3S$, 306.0907).

S-Pyrisulfoxin A [(+)-3]: white amorphous powder; $[\alpha]_D^{15}$ +51.5 (*c* 1, MeOH); UV(MeOH) λ_{max} (lg ε) 243 (4.37), 287 (4.13) nm; ECD (0.86 mM, MeOH) λ_{max} ($\Delta\varepsilon$) 207 (−17.2), 244 (−4.6), and 296 (+5.4) nm; ^{1}H NMR and ^{13}C NMR, see **Tables 2**, **3**, **Figures S33, S34**. HRESIMS *m/z* 292.0754 [M + H]$^+$ (calcd for $C_{13}H_{14}N_3O_3S$, 292.0750) (**Figure S31**).

TABLE 1 | ^{1}H Nuclear Magnetic Resonance (NMR) data of compounds **1**, (±)-**2**, and (±)-**2a** at 500 MHz.

No.	1 (CD$_3$OD)	(±)-2 (DMSO-d_6)	(±)-2 (CD$_3$OD)	(±)-2^a (DMSO-d_6)	(±)-2a^b (DMSO-d_6)
	δ_H (*J* in Hz)	δ_H (*J* in Hz)	δ_H (*J* in Hz)	δ_H (*J* in Hz)	δ_H (*J* in Hz)
3	8.01, s	7.38, s	7.15, s	7.36, s	8.03, s
4	–	–	–	–	–
4-OCH$_3$	4.05, s	–	–	–	4.04, s
5	–	–	–	–	–
5-SOCH$_3$	3.06, s	3.03, s	3.16, s	3.01, s	3.03, s
6	–	–	–	–	–
7	4.96, d (15.0)	4.71, m	4.91, m	4.72, m	4.65, dd (5.3, 15.8)
	4.92, d (15.0)				4.85, dd (6.0, 15.8)
NHCOCH$_3$	–	1.92, s	2.07, s	1.92, s	1.92, s
3′	8.46, dd (7.7)	8.32, d (7.8)	8.14, d (7.7)	8.31, d (7.1)	8.52, d (7.7)
4′	7.92, dd (7.7, 7.5)	7.96, dd (7.8, 7.5)	7.99, dd (7.7, 7.0)	7.98, dd (7.1, 6.0)	8.03, m
5′	7.42, dd (7.5, 4.4)	7.49, dd (7.5, 4.0)	7.54, dd (7.0, 4.0)	7.50, brs	7.53, dd (7.5, 5.0)
6′	8.64, d (4.4)	8.69, d (4.0)	8.75, d (4.0)	8.70, brs	8.73, brs
NH	–	8.49, brs	–	8.46, brs	8.33, brs

^{a}Synthetic compound; ^{b}Recorded at 600 MHz.

TABLE 2 | ^{1}H NMR data of compounds (±)-**3**, (±)-**4**, **13**, and (±)-**14** at 500 MHz.

No.	(±)-3 ^{a} (CD$_3$OD)	(±)-4 (CDCl$_3$)	13 (CDCl$_3$)	(±)-14 ^{a,b} (CDCl$_3$)
	δ_H (*J* in Hz)	δ_H (*J* in Hz)	δ_H (*J* in Hz)	δ_H (*J* in Hz)
3	8.14, s	8.31, s	8.01, s	8.05, s
4	–	–	–	–
4-OCH$_3$	4.15, s	4.17, s	4.10, s	4.12, s
5	–	–	–	–
5-SO/S-CH$_3$	3.15, s	3.11, s	2.38, s	2.44, s
6	–	–	–	–
7	8.44, s	–	6.09, s	6.36, s
7-OCH$_3$	–	–	3.56, s	3.56, s
NHCOCH$_3$	–	–	–	–
3′	8.49, d (8.0)	8.52, dd (8.0, 1.2)	8.56, d (8.0)	8.33, dd (7.8, 1.5)
4′	7.95, dd (8.0, 7.8)	7.89, ddd (8.0, 7.8, 1.8)	7.80, dd (8.0, 7.8)	7.80, ddd (7.8, 7.8, 1.5)
5′	7.49, dd (7.8, 5.0)	7.43, ddd (7.8, 4.6, 1.2)	7.31, dd (7.8, 4.8)	7.30, m (overlap)
6′	8.67, brs	8.68, dd (4.6 1.8)	8.65, d (4.8)	8.62, dd (4.5, 1.5)

^{a}Recorded at 600 MHz; ^{b}The δ_H values of H-8, H-12, and H-13–H-16 were 6.82 (brs, H-8), 5.22 (brs, H-12), 6.78 (dd, *J* = 7.5, 1.2 Hz, H-13), 7.32 (m, overlap, H-14), 6.90 (ddd, *J* = 7.9, 7.5, 1.2 Hz, H-15), and 7.96 (dd, *J* = 7.9, 1.1 Hz, H-16), respectively.

R-Pyrisulfoxin A [(−)-**3**]: white amorphous powder; $[\alpha]_D^{15}$ −40.7 (*c* 1, MeOH); UV(MeOH) λ_{max} (lg ε) 243 (4.37), 287 (4.13) nm; ECD (0.86 *m*M, MeOH) λ_{max} ($\Delta\varepsilon$) 207 (+11.7), 244 (+3.1), and 296 (−3.6) nm; ^{1}H NMR and ^{13}C NMR, see **Tables 2**, **3**, **Figures S33, S34**. HRESIMS *m/z* 292.0752 [M + H]$^+$ (calcd for C$_{13}$H$_{14}$N$_3$O$_3$S, 292.0750) (**Figure S32**).

S-Pyrisulfoxin B [(+)-**4**]: white amorphous powder; $[\alpha]_D^{14}$ +22.4 (*c* 0.25, MeOH); UV(MeOH) λ_{max} (lg ε) 240 (3.58), 289 (3.47) nm; ECD (0.92 *m*M, MeOH) λ_{max} ($\Delta\varepsilon$) 214 (−2.9), 243 (−2.1) and 293 (+1.8) nm; ^{1}H NMR and ^{13}C NMR, see **Tables 2**, **3**, **Figures S37, S38**. HRESIMS *m/z* 274.0650 [M + H]$^+$ (calcd for C$_{13}$H$_{12}$N$_3$O$_2$S, 274.0645) (**Figure S35**).

R-Pyrisulfoxin B [(−)-**4**]: white amorphous powder; $[\alpha]_D^{14}$ −15.2 (*c* 0.25, MeOH); UV(MeOH) λ_{max} (lg ε) 240 (3.58), 289 (3.47) nm; ECD (0.92 *m*M, MeOH) λ_{max} ($\Delta\varepsilon$) 214 (+5.3), 243 (+4.0) and 293 (−3.6) nm; ^{1}H NMR and ^{13}C NMR, see **Tables 2**, **3**, **Figures S37, S38**. HRESIMS *m/z* 274.0650 [M + H]$^+$ (calcd for C$_{13}$H$_{12}$N$_3$O$_2$S, 274.0645) (**Figure S36**).

Pyrisulfoxin E (**13**): white amorphous powder; UV(MeOH) λ_{max} (log ε) 226 (3.49), 287 (3.36) nm; ^{1}H NMR and ^{13}C NMR, see **Tables 2**, **3**. HRESIMS *m/z* 307.1118 [M + H]$^+$ (calcd for C$_{15}$H$_{19}$N$_2$O$_3$S, 307.1111).

S-Pyrisulfoxin F [(+)-**14**]: white amorphous powder; $[\alpha]_D^{25}$ +14.5 (*c* 0.5, MeOH); UV(MeOH) λ_{max} (log ε) 221 (2.49), 282

TABLE 3 | ^{13}C NMR data of compounds 1–4, (±)-2a, 13, and (±)-14 at 125 MHz.

No.	1 (CD$_3$OD)	(±)-2 (DMSO-d_6)	(±)-2 (CD$_3$OD)	(±)-2^a (DMSO-d_6)	(±)-2a^b (DMSO-d_6)	(±)-3^b (CD$_3$OD)	(±)-4^a (CDCl$_3$)	13 (CDCl$_3$)	(±)-14^{b,c} (CDCl$_3$)
	δ_C	δ_C	δ_C	δ_C	δ_C	δ_C	δ_C	δ_C	δ_C
2	160.2, C	Absent	Absent	Absent	158.3, C	160.9, C	161.7, C	absent	158.0, C
3	105.2, CH	111.3, C^d	114.1, C	111.1, C	103.6, CH	105.6, CH	107.0, CH	103.4, CH	103.8, CH
4	166.9, C	Absent	Absent	Absent	164.9, C	167.8, C	165.1, C	168.1, C^d	167.9, C
4-OCH$_3$	57.1, CH$_3$	–	–	–	57.2, CH$_3$	57.1, CH$_3$	57.4, CH$_3$	56.4, CH$_3$	56.7, CH$_3$
5	126.0, C	125.3, C^d	127.1, C^d	Absent	126.5, C	127.5, C	132.2, C	120.7, C^d	118.6, C
5-SO/S-CH$_3$	38.8, CH$_3$	38.6, CH$_3$	39.0, CH$_3$	38.9, CH$_3$	38.9, CH$_3$	38.5, CH$_3$	40.4, CH$_3$	18.3, CH$_3$	18.2, CH$_3$
6	161.0, C	154.8, C^d	absent	Absent	157.4, C	152.9, C	133.3, C	absent	156.6, C
7	64.6, CH$_2$	41.4, CH$_2^d$	37.7, CH$_2^d$	Absent	41.5, CH$_2$	148.3, CH	114.9, C	101.7, CH	65.7, CH
NHCOCH$_3$	–	22.5, CH$_3$ 170.4, C^d	22.3, CH$_3$ 174.9, C^d	22.4, CH$_3$ 170.5, C	23.4, CH$_3$ 169.9, C	–	–	–	–
7-OCH$_3$	–	–	–	–	–	–	–	54.8, CH$_3$	
2'	155.6, C	absent	absent	absent	154.5, C	155.6, C	153.3, C	155.7, C^d	154.9, C
3'	123.1, CH	121.1, CH	122.3, CH	121.1, CH	121.7, CH	123.2, CH	122.6, CH	122.2, CH	121.9, CH
4'	138.7, CH	137.6, CH	139.2, CH	137.7, CH	138.2, CH	138.8, CH	137.8, CH	137.1, CH	137.3, CH
5'	126.2, CH	125.0, CH	126.8, CH	125.1, CH	125.5, CH	126.3, CH	126.0, CH	124.2, CH	124.6, CH
6'	150.3, CH	149.3, CH	150.7, CH	149.3, CH	149.8, CH	150.3, CH	149.7, CH	149.0, CH	149.1, CH

^{a}Synthetic compound; ^{b}Recorded at 150 MHz; ^{c}The δ_C values of C-9–C-11 and C-13–C-16 were 165.2 (C, C-9), 117.4 (C, C-10), 147.2 (C, C-11), 115.6 (CH, C-13), 133.8 (CH, C-14), 119.9 (CH, C-15), and 128.6 (CH, C-16), respectively; ^{d}Absent in 1D NMR but present in 2D NMR.

(2.15) nm; ECD (1.3 mM, MeOH) λ_{max} ($\Delta\varepsilon$) 214 (+3.14), 230 (−2.42), 251 (−2.72), 269 (+0.09), 290 (−2.51), and 325 (+1.31) nm; ^{1}H NMR and ^{13}C NMR, see **Tables 2**, **3**. HRESIMS m/z 379.1222 [M + H]$^+$ (calcd for C$_{20}$H$_{19}$N$_4$O$_2$S, 379.1223).

R-Pyrisulfoxin F [(−)-**14**]: white amorphous powder; $[\alpha]_D^{25}$ −16.9 (c 0.5, MeOH); UV(MeOH) λ_{max} (log ε) 221 (2.49), 282 (2.15) nm; ECD (1.3 mM, MeOH) λ_{max} ($\Delta\varepsilon$) 212 (−2.81), 230 (+1.48), 251 (+1.66), 269 (−0.18), 290 (+1.77), and 325 (−0.95) nm; ^{1}H NMR and ^{13}C NMR, see **Tables 2**, **3**. HRESIMS m/z 379.1222 [M + H]$^+$ (calcd for C$_{20}$H$_{19}$N$_4$O$_2$S, 379.1223).

Oxidation of Compound 5 to (±)-2

Compound **5** (9.0 mg) was dissolved into 2.25 ml of THF and 0.45 ml of water. The mixture was cooled in an ice bath, and 120 μl of aqueous solution of potassium peroxomonosulfate (Oxone) (0.1 g/ml) was added dropwise. The resulting mixture was stirred at 0°C for 2.5 h. Then, 1 ml of aqueous solution of NaHCO$_3$ (pH 8) was added to quench the reaction. The reaction product was extracted by *n*-BuOH to afford 9.2 mg (96.8% yield) of (±)-**2**, which was identified by the same MS (**Figure S22**) and co-HPLC retention time (t_R 10.5 min, **Figure S39**) and NMR (**Figures S23, S24, Tables 1, 3**) to those of natural one.

Methylation of (±)-2 With TMS-CHN$_2$

Five milligram of (±)-**2** was dissolved in anhydrous MeOH (5 ml), and then 0.9 ml of TMS-CHN$_2$ (2.0 M in *n*-hexane) was added. After stirring for 2.5 h at room temperature (about 20°C), the reaction mixture was evaporated to dryness and prepared by semi-preparative HPLC on an ODS column (10%−100% MeCN-H$_2$O with 0.5‰ CF$_3$CO$_2$H) to yield (±)-**2a** (2.5 mg, t_R 5.36 min, 43.5% yield). (±)-**2a** was further separated into (+)-**2a** (1.0 mg,

t_R 10.8 min) and (−)-**2a** (1.0 mg, t_R 14.0 min) on a Chiral INC 5 u analytical column (35% EtOH/*n*-hexane).

4-*O*-Methylpyrisulfoxin D [(±)-**2a**]: white amorphous powder; UV(MeOH) λ_{max} (log ε) 221 (3.05), 248 (2.81), 289 (3.00) nm; IR (KBr) ν_{max} 3,444, 1,683, 1,574, 1,428, 1,383, 1,205, 1,136, 1,056, 800 cm^{-1}; ^{1}H NMR (600 MHz) and ^{13}C NMR (150 MHz), see **Tables 1**, **3**, **Figures S26–S30**. HRESIMS m/z 320.1070 [M + H]$^+$ (calcd for C$_{15}$H$_{18}$N$_3$O$_3$S, 320.1063) (**Figure S25**).

S-4-*O*-Methylpyrisulfoxin D [(+)-**2a**]: $[\alpha]_D^{25}$ +44.6 (c 0.5, MeOH); ECD (1.57 mM, MeOH) λ_{max} ($\Delta\varepsilon$) 217 (−7.8), 245 (−3.8) and 293 (+6.1) nm.

R-4-*O*-Methylpyrisulfoxin D [(−)-**2a**]: $[\alpha]_D^{25}$ −41.4 (c 0.5, MeOH); ECD (1.57 mM, MeOH) λ_{max} ($\Delta\varepsilon$) 217 (+6.2), 245 (+2.9) and 293 (−4.8) nm.

ECD Calculation

The calculations were performed by using the density functional theory (DFT) as carried out in the Gaussian 09 (Frisch et al., 2010). The preliminary conformational distributions search was performed by HyperChem 8.0 software. All ground-state geometries were optimized at the B3LYP/6-31G(d) level (Stephens et al., 2007) (**Tables S4–S6**). Time-dependent DFT (TDDFT) at B3LYP/6-31G(d) was employed to calculate the electronic excitation energies and rotational strengths in MeOH (Casida, 1995) (**Tables S7–S9**). The overall calculated ECD curves were weighted by Boltzmann distribution with a half-bandwidth of 0.30 eV and UV corrections of compounds (*S*)-**2**, (*R*)-**3**, and (*S*)-**14** were −15, 0, and 0 nm, respectively. The calculated ECD spectra were produced by SpecDis 1.70.1 software (Bruhn et al., 2017). Solvent effects of MeOH were evaluated at the same DFT level by use of the SCRF/PCM method (Cammi and Tomasi, 1995).

Cytotoxic Assays

The cytotoxic activities of compounds **1** and (±)-**2** were detected by CellTiter-Glo® (CTG) assay (He et al., 2019) against human colon carcinoma cell lines (HCT-116), lung cancer cell lines (A549, H1975, H1299, SPC-A1, H2228), breast cancer cell lines (MCF-7, BT474, MDA-MB-231, MDA-MB-468), glioblastoma cell line (U87, U251), leukemia cell lines (HL-60, MV-4-11, K562), ductal carcinoma cell line (HCC1954, HUCCT1), gastric cancer cell line (MKN-45), epidermoid carcinoma cell line (A431), liver cancer cell line (Hep3B), prostate cancer cell line (DU145), gastric carcinoma cell line (N87), rhabdomyoma cell line (A673), bone osteosarcoma cell line (143B), T cell lymphoma cell line (Karpass299), B16F10 (highly metastatic mouse melanoma cell line), as well as the human embryonic kidney-293F cell line (HEK-293F) and normal liver cell line (L02). Cells were cultured in Dulbecco's Modified Eagle Medium (DMEM) supplemented with 10% fetal bovine serum and 1% penicillin–streptomycin solution under a humidified atmosphere of 95% air and 5% CO_2 at 37°C. Ninety microliter of culture solution (containing fetal bovine serum) and 100 µl of cell suspension at a density of 2×10^3 cell/ml was plated in 96-well microtiter plates, allowed to attach overnight, and then exposed to 10 µl of drugs for 72 h within the final concentrations of 0.032, 0.16, 0.8, 4, 20, and 100 µM, respectively. Hundred microliter of the CTG solution was then added to each well and incubated for 10 min, and the absorbance was read at 500 nm on a Spectra Max Plus plate reader. Adriamycin was used as the positive control.

The cytotoxicities of compounds **3–12** against Jurkat, K562, MCF-7, and P6C cell lines were assayed by 3-(4,5-Dimethylthiazol-2-yl)-2,5-diphenyltetrazolium bromide (MTT) method (Mosmann, 1983). MCF-7 and P6C cell lines were grown in RPMI-1640 supplemented with 10% Fetal Bovine Serum (FBS) under a humidified atmosphere of 5% CO_2 and 95% air at 37°C, respectively. Cell suspension, 200 µl, at a density of 5×10^4 cell/ml was plated in 96-well microtiter plates and incubated for 24 h. Then, the samples to be tested (final concentration, 10 µM) were added to each well and further incubated for 72 h. Twenty microliter of MTT solution (5 mg/ml in IPMI-1640) was then added to each well and incubated for 4 h. Old medium containing MTT (150 µl) was then gently replaced by DMSO and pipetted to dissolve any formazan crystals formed. Absorbance was then determined on a Spectra Max Plus plate reader at 570 nm. Jurkat and K562 cell lines were grown in DMEM supplemented with 10% FBS, 2 mM L-glutamine, 100 U/ml penicillin and 100 g/ml streptomycin under a humidified atmosphere of 5% CO_2 at 37°C. The cells in the logarithmic growth phase were seeded in 96-well plates at 8,000 cells/well (180 ml/well). After 24 h at 37°C and 5% CO_2, the samples to be tested were added (final concentration, 10 µM) and three replicate wells were set for each concentration. The solvent control Dimethyl Sulfoxide (DMSO) was used in an amount of 0.1% of the maximum dose used in the test group. After 72 h of drug treatment at 37°C and 5% CO_2, 20 µl of MTT (5 mg/ml) was added and incubated for another 4 h. Then, 100 µl mixture of 10% SDS, 5% isopropanol and 12 mM HCl was added and incubated for 12–20 h. The optical density of each well at 570 nm was read by a microplate reader.

The cytotoxicities of compounds **3–12** against HT29, HCT-116, and BXPC-3 cell lines were assayed by SRB method (Skehan et al., 1990). They were cultured as K562 and Jurkat cell lines described above. The cells in the logarithmic growth phase were seeded in 96-well plates at 8,000 cells/well (180 ml/well). After 24 h in 5% CO_2 and 37°C, the samples to be tested were added (final concentration, 10 µM) and three replicate wells were set for each concentration. The solvent control DMSO was used in an amount of 0.1% of the maximum dose used in the test group. After 72 h of drug treatment at 37°C and 5% CO_2, 50% (m/v) ice-cold trichloroacetic acid was added to each well to fix the cells. After SRB staining, 150 µl/well of Tris solution was added and the optical density of each well at 540 nm was read in a microplate reader.

RESULTS AND DISCUSSION

Identification of Compounds

Pyrisulfoxin C (**1**) was obtained as white amorphous powder. The molecular formula of **1** was determined to be $C_{13}H_{14}N_2O_3S$ by HRESIMS (**Figure S5**) with one more oxygen atom than compound **9**. Analysis of the ^{1}H NMR data (**Table 1**, **Figure S6**) for **1** and comparison with reported data showed four signals at 8.46 (H-3′, d, $J = 7.7$ Hz), 7.92 (H-4′, dd, $J = 7.7, 7.5$ Hz), 7.42 (H-5′, dd, $J = 7.5, 4.4$ Hz), and 8.64 (H-6′, d, $J = 4.4$ Hz), which were assigned to a 2-substituted pyridine ring system, and one signal at 8.01 (H-3, s) assigned to a 2,4,5,6-tetrasubstituted pyridine ring system. Heteronuclear Multiple Bond Correlations (HMBC) (**Figure 2**, **Figure S10**) from H-3′ to C-2 and from H-3 to C-2' identified a 2,2′-bipyridine structure. The signal at $\delta_{C/H}$ 64.6/4.92&4.96 was assigned as a hydroxymethyl. In addition, two methyl singlets were observed, among which the signal at $\delta_{C/H}$ 57.1/4.05 was a methoxy and the one at $\delta_{C/H}$ 38.8/3.15 was assigned as a methylsulfinyl group (**Tables 1**, **3**, **Figures S7–S9**). These data were very similar to those of SF2738 C (**9**) (Yin et al., 2016) except for the methylsulfinyl signal ($\delta_{C/H}$ 38.8/3.15), indicating **1** as a methyl sulphoxide (**Figure 2**). The constitution of **1**, named as pyrisulfoxin C, was thus elucidated as 4-methoxy-5-methylsulfinyl-2,2′-bipyridine-6-methanol.

(±)-Pyrisulfoxin D [(±)-**2**] was obtained as a pair of racemate. Its molecular formula was assigned as $C_{14}H_{15}N_3O_3S$ from the HRESIMS peak at *m/z* 306.0916 $[M+H]^+$ (**Figure S11**), which has one more oxygen atom than compound **5**. Similar to **1**, proton signals measured in DMSO-d_6 at 8.32 (H-3′, d), 7.96 (H-4′, dd), 7.49 (H-5′, dd), 8.69 (H-6′, d), and 7.38 (H-3, s) (**Table 1**, **Figure S12**) were assigned to a 2,2′-bipyridine system. Besides the 2,2′-bipyridine core skeletons, its NMR (**Tables 1**, **3**, **Figures S12–S14**) displayed one NH signal at δ_H 8.49 (1H, brs), one methylene at δ_H 4.71, and one acetyl group at $\delta_{C/H}$ 22.5/1.92 and δ_C 170.4. And the key COSY correlation signals (**Figure 2**, **Figure S15**) of H-7 (δ_H 4.71, m, 2H) to NH (δ_H 8.49, brs, 1H) revealed the -CH_2-NH- group. The HMBC correlation signals (**Figure 2**, **Figure S16**) between both methyl protons (δ_H 1.92) and methylene protons (δ_H 4.71) with the carbonyl carbon (δ_C 170.4) established an (acetylamino)methyl group. These data are very similar to those of **5** (Ignacio et al., 2012) within the main

FIGURE 1 | Structures of compounds **1–3**, **13**, and **14**.

FIGURE 2 | Key ^{1}H-^{1}H COSY and HMBC correlations of **1**, (±)-**2**, and (±)-**2a**.
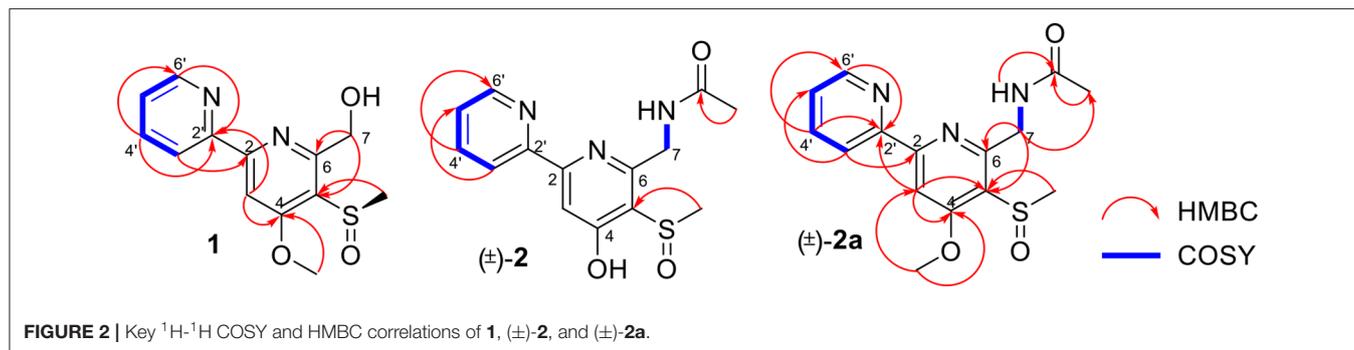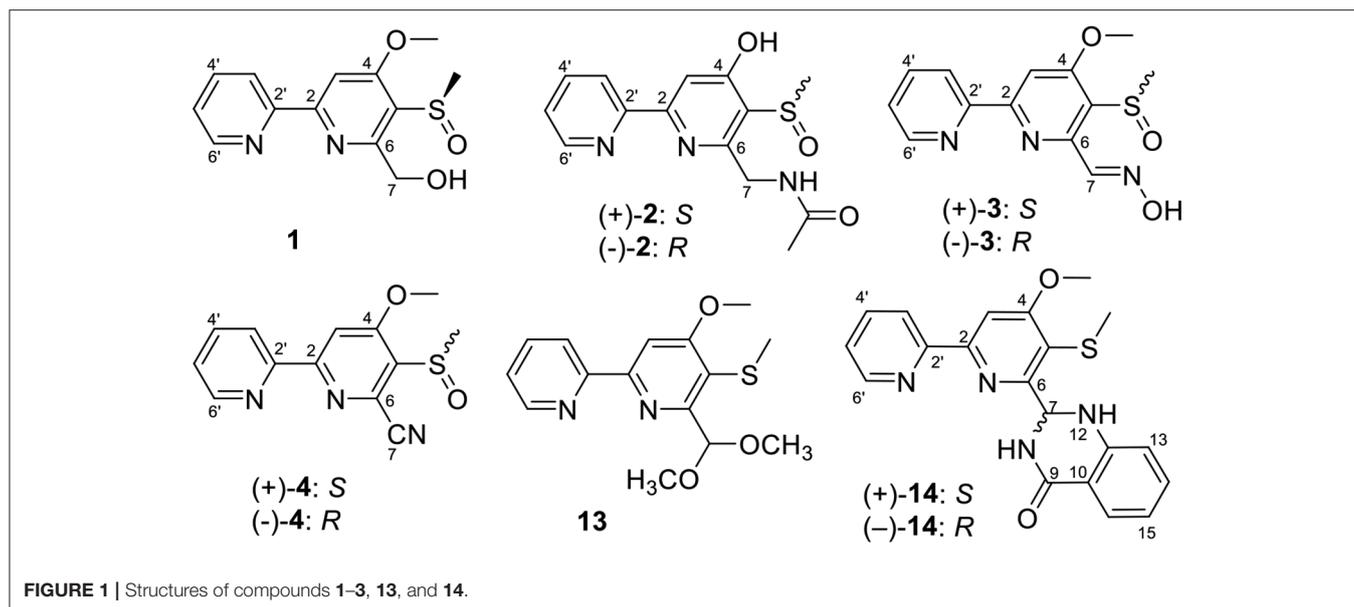
difference that the -SCH$_3$ protons' signal at δ_H 2.25 (3H, s) in **5** moved to δ_H 3.03 (3H, s) in (±)-**2**, indicating the existence of a -S(O)CH$_3$ group in (±)-**2**. Unexpectedly, three non-protonated carbon signals (C-2, C-4 and C-2′) were absent in both 1D and 2D NMR spectra of (±)-**2**, even after changing the solvent as MeOH-d_6 (**Table 3**, **Figures S17–S21**). To further confirm the constitution of (±)-**2**, (±)-**2** was prepared by oxidation of the known compound **5** with Oxone (**Scheme 1**). The product was identified by the same MS (**Figure S22**), the same co-HPLC retention times (t_R 10.5 min, **Figure S39**) and almost the same 1D NMR (**Figures S23, S24**, **Tables 1**, **3**) to the natural (±)-**2**. Therefore, the constitution of (±)-**2**, named as pyrisulfoxin D, was identified as *N*-[(4-hydroxy-5-methylsulfinyl-2,2′-bipyridin-6-yl)methyl] acetamide. However, the carbon signals of C-2, C-4, C-5, C-6, C-7, and C-2′ were neither absent in the ^{13}C NMR spectrum of the synthetic (±)-**2** due to the coinfluence of 4-OH and 3-S(O)CH$_3$. In order to verify this hypothesis, a new 4-*O*-methyl derivative [(±)-**2a**] was prepared from the methylation of (±)-**2** by TMS-CHN$_2$ (**Scheme 1**) and identified by HRESIMS (**Figure S25**) as well as 1D and 2D NMR spectra (**Figure 2**, **Figures S26–S30**). As expected, these non-hydrogenated carbon signals were present in the ^{13}C NMR spectrum of (±)-**2a** (**Figure S27, Table 3**).

Compared to other natural products, the absolute configuration of the chiral sulfoxide is less concerned. Apart from X-ray single crystal diffraction, sulfoximine NMR method (Kusumi et al., 2006), and vibrational circular dichroism (VCD) spectroscopy (Stephens et al., 2001), the ECD spectroscopy was widely used to determine the absolute configuration of the chiral sulfoxide (Cho and Plapp, 1998; Donnoli et al., 2003). To determine the absolute configurations, the racemic pyrisulfoxin D [(±)-**2**], pyrisulfoxin A [(±)-**3**], pyrisulfoxin B [(±)-**4**] and (±)-4-*O*-methyl pyrisulfoxin D [(±)-**2a**] were first separated on a chiral column into their optically pure isomers (+)-**2** and (−)-**2** (**Figure S1**), (+)-**3** and (−)-**3** (**Figure S2**), (+)-**4** and (−)-**4** (**Figure S3**), as well as (+)-**2a** and (−)-**2a** (**Figure S4**), respectively. Then, ECD spectra were measured and the results indicated that (+)-**2**, (+)-**2a**, (+)-**3**, and (+)-**4** displayed strong negative Cotton effects, while (−)-**2**, (−)-**2a**, (−)-**3**, and (−)-**4** showed strong positive Cotton effects around λ_{max} 210–220 nm (**Figures 3–5**). The Cotton effects around λ_{max} 210–220 nm that arose from the exciton-couple of the chromophores S=O (n→ π*) and pyridine (π → π*) could be used to identify the absolute configuration of aryl methyl sulfoxides, which the positive and negative effects were correlated to the *R*- and *S*-configurations, respectively (Cho and Plapp, 1998). To confirm

SCHEME 1 | The oxidation of **5** and the methylation of (±)-**2** into (±)-**2a**.

FIGURE 3 | Experimental and calculated electronic circular dichroism (ECD) spectra of S(+)-**2** and R(−)-**2** in MeOH.

FIGURE 4 | Experimental and calculated ECD spectra of S(+)-**3** and R(−)-**3** in MeOH.
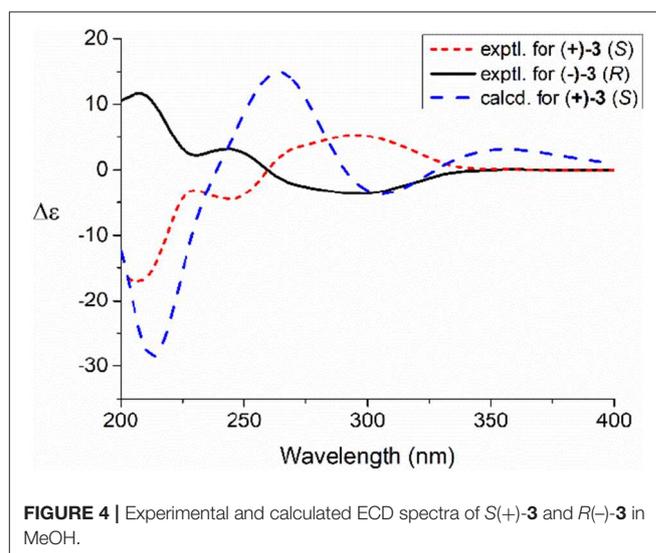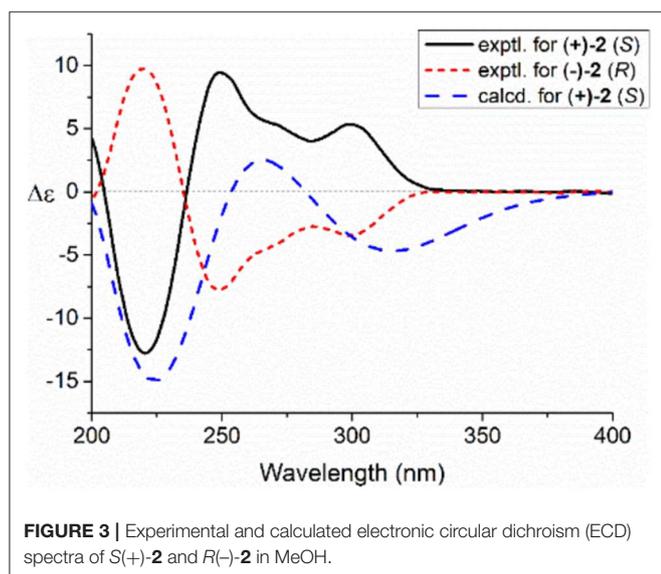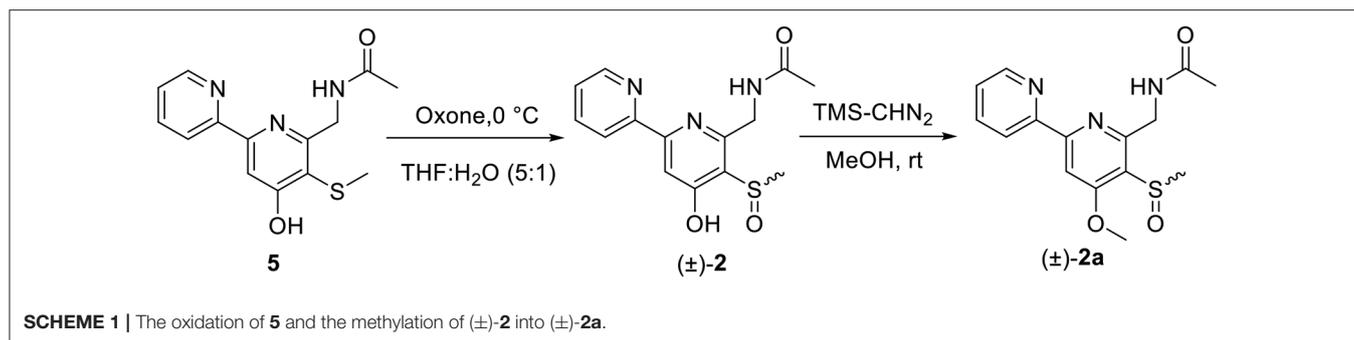
the deduction, we further calculated the ECD spectra of the optically pure compounds (S)-**2** and (R)-**3** by means of DFT at B3LYP/6-31G(d) level. The calculated ECD spectra (S)-**2** and (R)-**3** matched well with the experimental ECD spectra of (+)-**2** and (−)-**3**, which showed Cotton effects around λ_{max} ($\Delta\varepsilon$) 221 (−12.8), 250 (+9.4) and 300 (+5.3) nm, and 207 (+11.7), 244 (+3.1) and 296 (−3.6) nm, respectively (**Figures 3**, **4**), further indicating the configurations of (+)-**2** and (−)-**3** as S- and R-, respectively. Thus, the absolute configurations of (−)-**2** and (+)-**3** were respectively determined as R- and S-. As shown in **Figure 5**, the experimental ECD spectra of **1**, (−)-**2a**, and (−)-**4** were similar to that of (−)-**3**, but opposite to those of (+)-**3**, (+)-**2a**, and (+)-**4**. Thus, the absolute configurations of **1**, (−)-**2a**, (−)-**4**, (+)-**2a**, and (+)-**4** were determined to be R-, R-, R-, S-, and S-, respectively.

Pyrisulfoxin E (**13**) was obtained as white amorphous powder. HRESIMS showed the protonated molecular ion peak at *m/z* 307.1118 [M+H]$^+$, indicating a molecular formula $C_{15}H_{18}N_2O_3S$ (**Figure S40**). ^{1}H NMR signals at 8.56 (H-3′, d), 7.80 (H-4′, dd), 7.31 (H-5′, dd), 8.65 (H-6′, d) (**Table 2**, **Figure S41**), and 8.01 (H-3, s) were assigned to a 4,5,6-tetrasubstituted 2,2′-bipyridine ring system. What more, ^{1}H-^{1}H

COSY correlative signals of H-3′/H-4′/H-5′/H-6′ (**Figure S44**) and HMBC correlative signals from H-2 to C-2′ (**Figure S45**) verified that. Three methoxy and one methylthio signals were observed at $\delta_{C/H}$ 56.4/4.10 (OCH$_3$-4), 54.8/3.56 (OCH$_3$-7), and $\delta_{C/H}$ 18.3/2.38 (SCH$_3$-5), respectively (**Tables 2**, **3**, **Figures S41–S43**). These data indicated that compound **13** also contained the same 6-substituted 4-methoxy-5-methylthio-2,2′-bipyridine skeleton as SF2738 C (**9**) (Yin et al., 2016). The rest methine signal at $\delta_{C/H}$ 101.7/6.09 (CH-7), along with its HMBC correlation with the two methoxy protons at δ_H 3.56, suggested a methylal moiety that was linked to C-6 of the 2,2′-bipyridine nucleus from the key HMBC correlations of H-7 (δ_H 6.09), H-3 (δ_H 8.01), and methylthio proton (δ_H 2.38) to C-5 (δ_C 120.7) (**Figure 6**, **Figure S45**). Thus, compound **13**, named as pyrisulfoxin E, was elucidated as 6-dimethoxymethyl-4-methoxy-5-methylthio-2,2′-bipyridine.

Pyrisulfoxin F [(±)-**14**] was obtained as white amorphous powder. The protonated molecular ion peak at *m/z* 379.1222 [M+H]$^+$ in HRESIMS indicating the molecular formula $C_{20}H_{18}N_4O_2S$ (**Figure S46**). Similar to those of **13**, ^{1}H NMR signals at δ_H 8.33 (H-3′, dd), 7.80 (H-4′, ddd), 7.30 (H-5′, m), 8.62 (H-6′, dd), 8.05 (H-3, s), 4.12 (3H, OCH$_3$-4), and 2.44 (3H, SCH$_3$-5) (**Table 2**, **Figure S47**) indicated

the same 6-substituted 4-methoxy-5-methylthio-2,2′-bipyridine skeleton. ^{1}H-^{1}H COSY correlative signals of H-3′/H-4′/H-5′/H-6′ (**Figure S50**) and HMBC correlative signals from H-3 to C-2′ (δ_C 154.9), H-3 and OCH$_3$-4 to C-4 (δ_C 167.9), as well as H-3 and SCH$_3$-5 to C-5 (δ_C 118.6) (**Figure S51**) confirmed the deduction. Apart from this moiety, another four *ortho*-disubstituted benzene protons observed at δ_H 6.78 (H-13, dd), 7.32 (H-14, m), 6.90 (H-15, ddd), and 7.96 (H-16, dd), which was further supported by ^{1}H-^{1}H COSY correlations of H-13/H-14/H-15/H-16 (**Figure 6**, **Figure S50**). The rest signals were observed at δ_H 5.22 (NH-12) and 6.82 (NH-8), δ_{C-9} 165.2 (carbonyl) and $\delta_{C/H}$ 65.7/6.36 (CH-7) (**Tables 2, 3, Figures S47–S49**) along with the ^{1}H-^{1}H COSY correlations of H-8/H-7/H-12 (**Figure S50**) and the HMBC correlations of H-7 (δ_H 6.36) and H-14 (δ_H 7.32) to C-11 (δ_C 147.2), H-12 (δ_H 5.22) and H-13 (δ_H 6.78) to C-10 (δ_C 117.4), and H-16 (δ_H 7.96) to C-9 (δ_C 165.2) and C-11 (**Figure 6**, **Figure S51**). These data implied a 2-substituted 2,3-dihydroquinazolin-4(1H)-one moiety. Thus, the 6-substituted 4-methoxy-5-methylthio-2,2′-

bipyridine and 2-substituted 2,3-dihydroquinazolin-4(1H)-one moieties connected together to form the constitution of racemic **14** (**Figure 1**), which was further separated on a chiral column into optically pure isomers (+)-**14** and (−)-**14** (**Figure S52**). ECD calculation of (*S*)-**14** at B3LYP/6-31G(d) level was used to determine the absolute configurations of the optically pure compounds. The results matched well with the experimental ECD spectrum of (+)-**14** that showed Cotton effects around λ_{max} ($\Delta\varepsilon$) 214 (+3.14), 230 (−2.42), 251 (−2.72), 269 (+0.09), 290 (−2.51), and 325 (+1.31) nm (**Figure 7**). Therefore, (+)-**14** was elucidated as *S*- configuration while (−)-**14** as *R*-configuration.

Biological Activity

Compounds **1**–**14** were evaluated for cytotoxic activity against a panel of human cancer cell lines by MTT, SRB, and CTG methods. As shown in **Table 4**, racemic (±)-**2** displayed a broad spectrum of cytotoxic activities against 26 cancer cell lines with IC$_{50}$ values ranging from 0.92 to 9.71 μM, while compound **1**

FIGURE 5 | ECD spectra of **1**, *R*(−)-**3** and *R*(−)-**4** in MeOH.

FIGURE 7 | Experimental and calculated ECD spectra of *S*(+)-**14** and *R*(−)-**14** in MeOH.

FIGURE 6 | Key ^{1}H-^{1}H COSY and HMBC correlations of **13** and (±)-**14**.
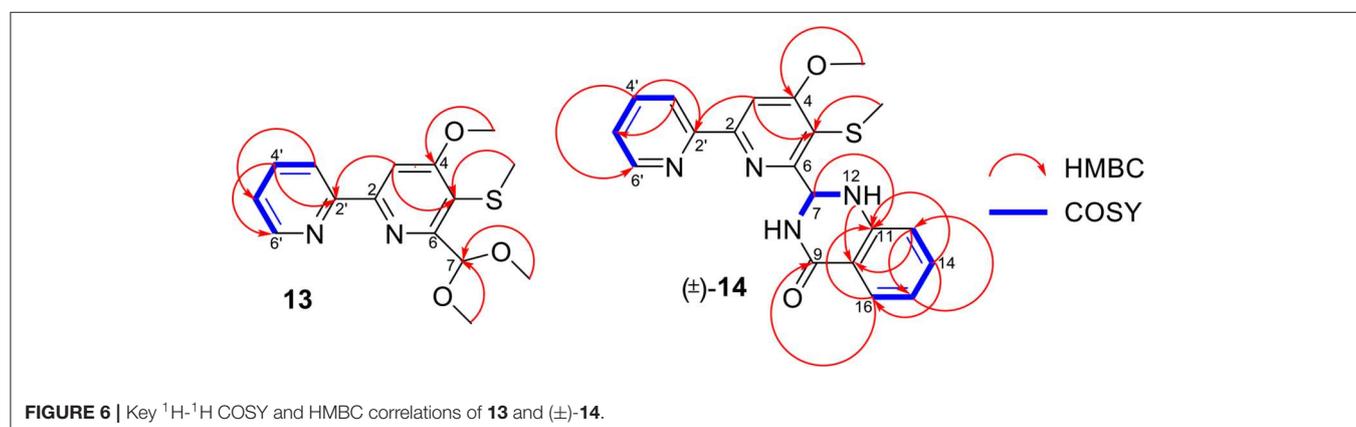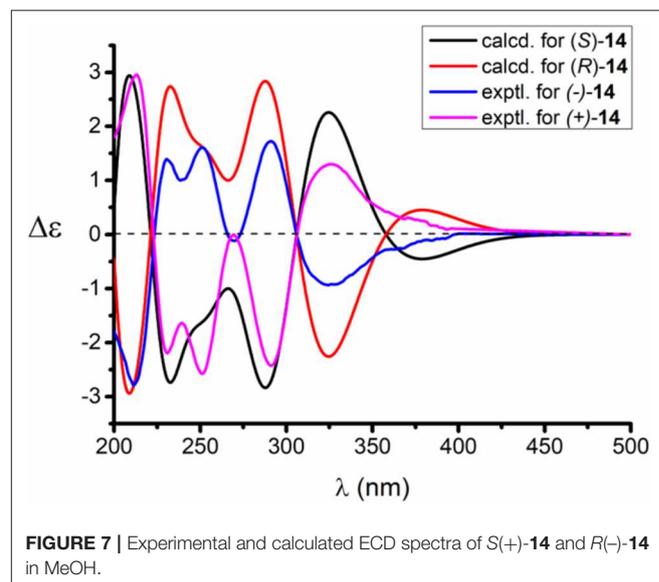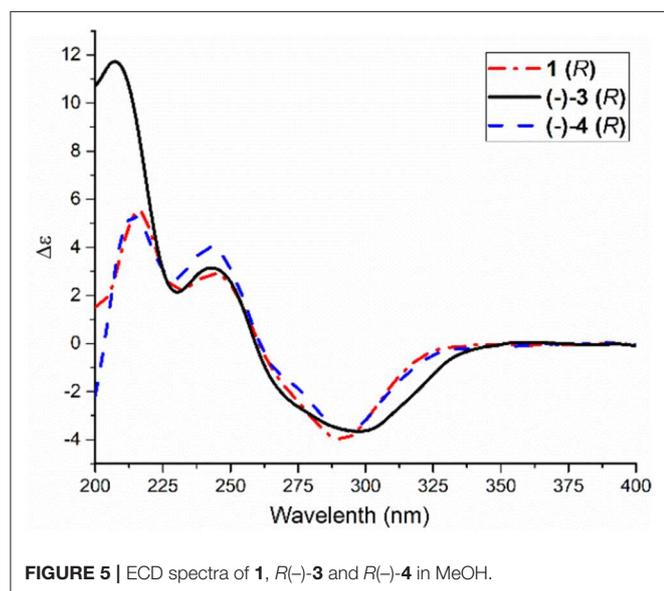
TABLE 4 | Cytotoxicity of **1**[a] and (±)-**2**[b] against cancer and normal cell lines (IC$_{50}$, μM).

Cell lines	A431	BT474	MDA-MB-468	U251	HCC1954	MCF-7	MKN-45	Hep3B	H1975
(±)-**2**	4.63	8.24	1.31	4.79	2.14	5.78	4.88	4.42	2.55
Adriamycin[c]	0.17	1.94	>100	0.19	0.048	0.10	0.19	17.58	0.091
Cell lines	**A673**	**H2228**	**MDA-MB-231**	**U87**	**Karpass299**	**HL60**	**MV-4-11**	**N87**	**H1299**
(±)-**2**	6.90	8.05	0.92	3.67	3.13	3.18	9.71	7.46	7.38
Adriamycin	0.13	0.097	0.18	0.12	0.39	0.21	0.16	0.12	0.49
Cell lines	**A549**	**K562**	**HCT-116**	**143B**	**B16F10**	**SPC-A1**	**HUCCT1**	**DU145**	**L02**
(±)-**2**	4.18	5.92	2.45	8.39	7.74	7.83	7.91	4.51	>100
Adriamycin	0.099	0.018	0.10	0.095	0.015	0.19	0.051	0.048	0.096

[a] The IC$_{50}$ values for **1** against N87 and other 26 cell lines were 8.09 μM and >100 μM, respectively. [b] The IC$_{50}$ for **2** against HEK-293F was >100 μM. [c] Positive control with an IC$_{50}$ value of 0.050 μM against HEK-293F cells.

TABLE 5 | Cytotoxicity of (±)-**3**, **7**, **8**, and **14** against cancer cell lines (IC$_{50}$, μM).

Cell lines	HCT-116	HT-29	P6C	BXPC-3	K562	Jurkat	MCF-7
(±)-**3**	0.73	0.83	3.2	1.6	13.0	NT[a]	NT
7	0.048	0.095	0.60	0.28	10.0	NT	1.6
8	0.10	0.20	0.30	0.49	8.4	13.7	1.8
R(+)-**14**	NA[c]	NT	NT	NT	NA	NT	10.4
S(−)-**14**	14.7	NT	NT	NT	NA	NT	NA
Adriamycin[b]	0.21	0.16	0.65	0.032	0.25	0.44	0.86

[a] NT, not tested, [b] Positive control, [c] NA, no activity.

showed a selective cytotoxicity against human gastric carcinoma cell line (N87) with an IC$_{50}$ value of 8.09 μM. As shown in **Table 5**, compounds **7**, **8**, and (±)-**3** showed cytotoxicity against human colorectal cancer (CRC) cell lines (HCT-116, HT-29, and P6C) and human pancreatic cancer cell line (BXPC-3) with IC$_{50}$ values ranging from 0.048 to 3.2 μM, while compounds **7** and **8** and *S*(+)-**14** also showed cytotoxicity against human breast cancer cell line (MCF-7) with IC$_{50}$ values of 1.6, 1.8, and 10.4 μM, respectively. The new compound *R*(−)-**14** showed inhibitory activity against HCT-116 with IC$_{50}$ of 14.7 μM. The results indicated that 6-oxime group or 6-acetylaminomethyl and 5-methylsulfinyl substitutions might be beneficial to the cytotoxicity of these 2,2′-bipyridine derivatives. Also, 6-oxime substituted 2,2′-bipyridine derivatives [(±)-**3**, **7**, and **8**] may have high selectivity against human CRC cells, indicating their potential use in the development of anti-CRC drugs.

CONCLUSIONS

Six new optically active caerulomycin compounds were obtained from two solid cultures of *Streptomyces albolongus* EA12432

endophytic with *Aconitum carmichaeli*. The racemic pyrisulfoxin D [(±)-**2**] showed broad-spectrum cytotoxic activities against cancer cell lines with the IC$_{50}$ values of 0.92–9.71 μM, while *R*-Pyrisulfoxin C (**1**), *S*-pyrisulfoxin F [(+)-**14**], and *R*-pyrisulfoxin F [(−)-**14**] showed a selective cytotoxicity against N87, MCF-7, and HCT-116 cancer cell lines with the IC$_{50}$ values of 8.09, 10.4, and 14.7 μM, respectively.

DATA AVAILABILITY STATEMENT

The raw data supporting the conclusions of this article will be made available by the authors, without undue reservation, to any qualified researcher.

AUTHOR CONTRIBUTIONS

All authors listed have made a substantial, direct and intellectual contribution to the work, and approved it for publication.

ACKNOWLEDGMENTS

SUPPLEMENTARY MATERIAL

The Supplementary Material for this article can be found online at: https://www.frontiersin.org/articles/10.3389/fchem.2020.00248/full#supplementary-material

REFERENCES

Ambavane, V., Tokdar, P., Parab, R. R., Sreekumar, E. S., Mahajan, G., Mishra, P. D., et al. (2014). Caerulomycin a–an antifungal compound isolated from marine actinomycetes. *Adv. Microbiol.* 4, 567–578. doi: 10.4236/aim.2014.49063

Bruhn, T., Schaumlöffel, A., Hemberger, Y., and Pescitelli, G. (2017). *SpecDis, Version 1.70.1, Berlin*. Available online at: https://specdissoftware.jimdo.com

Bu, Y. Y., Yamazaki, H., Ukai, K., and Namikoshi, M. (2014). Anti-mycobacterial nucleoside antibiotics from a marine-derived *Streptomyces* sp. TPU1236A. *Mar. Drugs* 12, 6102–6112. doi: 10.3390/md12126102

Cammi, R., and Tomasi, J. (1995). Remarks on the use of the apparent surface charges (ASC) methods in solvation problems: iterative versus matrix-inversion procedures and the renormalization of the apparent charges. *J. Comp. Chem.* 16, 1449–1458. doi: 10.1002/jcc.540161202

Casida, M. E. (1995). "Recent advances in computational chemistry," in *Recent Advances in Density Functional Methods*, *Part I*, ed D. P. Chong (Singapore: World Scientific), 155–192.

Cho, H., and Plapp, B. V. (1998). Specificity of alcohol dehydrogenases for sulfoxides. *Biochemistry* 37, 4482–4489. doi: 10.1021/bi9727040

Donnoli, M. I., Giorgio, E., Superchi, S., and Rosini, C. (2003). Circular dichroism spectra and absolute configuration of some aryl methyl sulfoxides. *Org. Biomol. Chem.* 1, 3444–3449. doi: 10.1039/b307017d

Edmands, W. M. B., Gooderham, N. J., Holmes, E., and Mitchell, S. C. (2013). S-Methyl-L-cysteine sulphoxide: the Cinderella phytochemical? *Toxicol. Res.* 2, 11–22. doi: 10.1039/C2TX20030A

Frisch, M. J., Trucks, G. W., Schlegel, H. B., Scuseria, G. E., Robb, M. A., Cheeseman, J. R., et al. (2010). *Gaussian 09, Revision B.01*. Wallingford, CT: Gaussian, Inc.

Fu, P., Liu, P., Li, X., Wang, Y., Wang, S., Hong, K., et al. (2011a). Cyclic bipyridine glycosides from the marine-derived actinomycete *Actinoalloteichus cyanogriseus* WH1-2216-6. *Org. Lett.* 13, 5948–5951. doi: 10.1021/ol202245s

Fu, P., Wang, S., Hong, K., Li, X., Liu, P., Wang, Y., et al. (2011b). Cytotoxic bipyridines from the marine-derived actinomycete *Actinoalloteichus cyanogriseus* WH1-2216-6. *J. Nat. Prod.* 74, 1751–1756. doi: 10.1021/np200258h

Fu, P., Zhu, Y., Mei, X., Wang, Y., Jia, H., Zhang, C., et al. (2014). Acyclic congeners from *Actinoalloteichus cyanogriseus* provide insights into cyclic bipyridine glycoside formation. *Org. Lett.* 16, 4264–4267. doi: 10.1021/ol5019757

Fukaya, M., Nakamura, S., Nakagawa, R., Nakashima, S., Yamashita, M., and Matsuda, H. (2017). Rare sulfur-containing compounds, kujounins A_1 and A_2 and *Allium* sulfoxide A_1, from *Allium fistulosum* 'Kujou'. *Org. Lett.* 20, 28–31. doi: 10.1021/acs.orglett.7b03234

Funk, A., and Divekar, P. V. (1959). Caerulomycin, a new antibiotic from *Streptomyces caeruleus* Baldacci: I. *production, isolation, assay, and biological properties*. *Can. J. Microbiol.* 5, 317–321. doi: 10.1139/m59-039

Gomi, S., Amano, S., Sato, E., Miyadih, S., and Kodama, Y. (1994). Novel antibiotics SF2738A, B and C, and their analogs produced by *Streptomyces* sp. *J. Antibiot.* 47, 1385–1394. doi: 10.7164/antibiotics.47.1385

Gurram, R. K., Kujur, W., Maurya, S. K., and Agrewala, J. N. (2014). Caerulomycin A enhances transforming growth factor-β (TGF-β)-Smad3 protein signaling by suppressing interferon-γ (IFN-γ)-signal transducer and activator of transcription 1 (STAT1) protein signaling to expand regulatory T cells (Tregs). *J. Biol. Chem.* 289, 17515–17528. doi: 10.1074/jbc.M113.545871

Hamada, T., Matsunaga, S., Yano, G., and Fusetani, N. (2005). Polytheonamides A and B, Highly cytotoxic, linear polypeptides with unprecedented structural features, from the marine sponge, *Theonella s winhoei*. *J. Am. Chem. Soc.* 127, 110–118. doi: 10.1021/ja045749e

He, W., Xu, Y., Fu, P., Zuo, M., Liu, W., Jiang, Y., et al. (2019). Cytotoxic indolyl diketopiperazines from the *Aspergillus* sp. GZWMJZ-258, endophytic with the medicinal and edible plant *Garcinia multiflora*. *J. Agric. Food Chem.* 67, 10660–10666. doi: 10.1021/acs.jafc.9b04254

Ignacio, G. L., Natalia, M. V., Alberto, S. G. C., Javier, G. S., Alfredo, F. B., Carmen, M. F., et al. (2012). *Colymycin derivatives*. Patent WO 2012/093192 A1. Available online at: https://lens.org/018-426-226-645-154

Imae, Y., Takada, K., Okada, S., Ise, Y., Yoshimura, H., Morii, Y., et al. (2013). Isolation of ciliatamide D from a marine sponge *Stelletta* sp. *and a reinvestigation of the configuration of ciliatamide A*. *J. Nat. Prod.* 76, 755–758. doi: 10.1021/np300878b

Kara, M., Asano, K., Kawamoto, I., Takiouchi, T., Katsumata, S., Takahashi, K. I., et al. (1989). Leinamycin, a new antitumor antibiotic from Streptomyces; producing organism, fermentation and isolation. *J. Antibiot.* 42, 1768–1774. doi: 10.7164/antibiotics.42.1768

Kobayashi, J. I., Nakamura, T., and Tsuda, M. (1996). Hymenamide F, new cyclic heptapeptide from marine sponge *Hymeniacidon* sp. *Tetrahedron* 52, 6355–6360. doi: 10.1016/0040-4020(96)00281-5

Kujur, W., Gurram, R. K., Haleem, N., Maurya, S. K., and Agrewala, J. N. (2015). Caerulomycin A inhibits Th2 cell activity: a possible role in the management of asthma. *Sci. Rep.* 5:15396. doi: 10.1038/srep15396

Kujur, W., Gurram, R. K., Maurya, S. K., Nadeem, S., Chodisetti, S. B., Khan, N., et al. (2017). Caerulomycin A suppresses the differentiation of naïve T cells and alleviates the symptoms of experimental autoimmune encephalomyelitis. *Autoimmunity* 50, 317–328. doi: 10.1080/08916934.2017.1332185

Kusumi, T., Ooi, T., Ohkubo, Y., and Yabuuchi, T. (2006). The modified Mosher's method and the sulfoximine method. *Bull. Chem. Soc. Jpn.* 79, 965–980. doi: 10.1246/bcsj.79.965

Lake, R. J., Brennan, M. M., Blunt, J. W., Munro, M. H., and Pannell, L. K. (1988). Eudistomin K sulfoxide-an antiviral sulfoxide from the New Zealand ascidian *Ritterella sigillinoides*. *Tetrahedron Lett.* 29, 2255–2256. doi: 10.1016/S0040-4039(00)86725-8

Lee, J. H., Kim, E., Choi, H., and Lee, J. (2017). Collismycin C from the micronesian marine bacterium *Streptomyces* sp. MC025 inhibits *Staphylococcus aureus* biofilm formation. *Mar. Drugs* 15:387. doi: 10.3390/md15120387

Lim, C. L., Nogawa, T., Uramoto, M., Okano, A., Hongo, Y., Nakamura, T., et al. (2014). RK-1355A and B, novel quinomycin derivatives isolated from a microbial metabolites fraction library based on NPPlot screening. *J. Antibiot.* 67, 323–329. doi: 10.1038/ja.2013.144

Mau, C. M., Nakao, Y., Yoshida, W. Y., Scheuer, P. J., and Kelly-Borges, M. (1996). Waiakeamide, a cyclic hexapeptide from the sponge *Ircinia dendroides*. *J. Org. Chem.* 61, 6302–6304. doi: 10.1021/jo960771e

Mehler, A. H. (1956). Formation of picolinic and quinolinic acids following enzymatic oxidation of 3-hydroxyanthranilic acid. *J. Biol. Chem.* 218, 241–254.

Mei, X., Lan, M., Cui, G., Zhang, H., and Zhu, W. (2019). Caerulomycins from *Actinoalloteichus cyanogriseus* WH1-2216-6: isolation, identification and cytotoxicity. *Org. Chem. Front.* 6, 3566–3574. doi: 10.1039/C9QO00685K

Mosmann, T. (1983). *Rapid colorimetric assay for cellular growth and survival: application to proliferation and cytotoxicity assays. J. Immunol. Methods* 65, 55–63. doi: 10.1016/0022-1759(83)90303-4

Murata, O., Shigemori, H., Ishibashi, M., Sugama, K. O., Hayashi, K., and Kobayashi, J. I. (1991). Eudistomidins E and F, new β-carboline alkaloids from the okinawan marine tunicate *Eudistoma glaucus*. *Tetrahedron Lett.* 32, 3539–3542. doi: 10.1016/0040-4039(91)80827-S

Nohara, T., Fujiwara, Y., Ikeda, T., Murakami, K., Ono, M., Nakano, D., et al. (2013). Cyclic sulfoxides garlicnins B_2, B_3, B_4, C_2, and C_3 from *Allium sativum*. *Chem. Pharm. Bull.* 61, 695–699. doi: 10.1248/cpb.c13-00082

Nohara, T., Kiyota, Y., Sakamoto, T., Manabe, H., Ono, M., Ikeda, T., et al. (2012). Garlicnins B_1, C_1, and D, from the fraction regulating macrophage activation of *Allium sativum*. *Chem. Pharm. Bull.* 60, 747–751. doi: 10.1248/cpb.60.747

Radulović, N. S., Miltojević, A. B., Stojković, M. B., and Blagojević, P. D. (2015). New volatile sulfur-containing compounds from wild garlic (*Allium ursinum* L., Liliaceae). *Food Res. Int.* 78, 1–10. doi: 10.1016/j.foodres.2015.11.019

Rashid, M. A., Gustafson, K. R., Boswell, J. L., and Boyd, M. R. (2000). Haligramides A and B, two new cytotoxic hexapeptides from the marine sponge *Haliclona nigra*. *J. Nat. Prod.* 63, 956–959. doi: 10.1021/np000051+

Schumacher, R. W., and Davidson, B. S. (1995). Didemnolines A-D, new N9-substituted β-carbolines from the marine ascidian *Didemnum* sp. *Tetrahedron* 51, 10125–10130. doi: 10.1016/0040-4020(95)00594-X

Sera, Y., Adachi, K., Fujii, K., and Shizuri, Y. (2003). A new antifouling hexapeptide from a Palauan sponge, *Haliclona* sp. *J. Nat. Prod.* 66, 719–721. doi: 10.1021/np020271i

Shindo, K., Yamagishi, Y., Okada, Y., and Kawai, H. (1994). Collismycins A and B, novel non-steroidal inhibitors of dexamethasone-glucocorticoid receptor binding. *J. Antibiot.* 47, 1072–1074. doi: 10.7164/antibiotics.47.1072

Skehan, P., Storeng, R., Scudiero, D., Monks, A., Mcmahon, J., Vistica, D., et al. (1990). New colorimetric cytotoxicity assay for anticancer-drug screening. *J. Natl. Cancer Inst.* 82, 1107–1112. doi: 10.1093/jnci/82.13.1107

Stephens, P. J., Aamouche, A., Devlin, F. J., Superchi, S., Donnoli, M. I., and Rosini, C. (2001). Determination of absolute configuration using vibrational circular dichroism spectroscopy: the chiral sulfoxide 1-(2-methylnaphthyl)

methyl sulfoxide. *J. Org. Chem.* 66, 3671–3677. doi: 10.1021/jo0 01403k

Stephens, P. J., Pan, J. J., and Krohn, K. (2007). Determination of the absolute configurations of pharmacological natural products via density functional theory calculations of vibrational circular dichroism: the new cytotoxic iridoid prismatomerin. *J. Org. Chem.* 72, 7641–7649. doi: 10.1021/jo0 71183b

Takada, K., Irie, R., Suo, R., and Matsunaga, S. (2017). Resolution of the confusion in the assignments of configuration for the ciliatamides, acylated dipeptides from marine sponges. *J. Nat. Prod.* 80, 2845–2849. doi: 10.1021/acs.jnatprod.7b00684

Thornburg, C. C., Cowley, E. S., Sikorska, J., Shaala, L. A., Ishmael, J. E., Youssef, D. T., et al. (2013). Apratoxin H and apratoxin A sulfoxide from the Red Sea cyanobacterium *Moorea producens. J. Nat. Prod.* 76, 1781–1788. doi: 10.1021/np4004992

Tsuge, N., Furihata, K., Shin-ya, K., Hayakawa, Y., and Seto, H. (1999). Novel antibiotics pyrisulfoxin A and B produced by *Streptomyces californicus. J. Antibiot.* 52, 505–507. doi: 10.7164/antibiotics. 52.505

Yin, H., Lin, J., and Chu, Y. (2016). Antifungal secondary metabolites produced by an endophytic actinobacteria isolate EA12432 from *Aconitum carmichaeli. Chin. J. Antibiot.* 41, 653–657. doi: 10.13461/j.cnki.cja.005761